Journal of Chromatography A, 1218 (2011) 6464–6475

Contents lists available at ScienceDirect

Journal of Chromatography A

journal homepage: www.elsevier.com/locate/chroma

Synthesis and characterization of surface modified SBA-15 silica materials and their application in chromatography

Tahira Yasmin[a,*], Klaus Müller[a,b]

[a] Institut für Physikalische Chemie, Universität Stuttgart, Pfaffenwaldring 55, D-70569 Stuttgart, Germany
[b] Dipartimento di Ingegneria dei Materiali e Tecnologie Industriali, Università degli Studi di Trento, via Mesiano 77, I-38123 Trento, Italy

ARTICLE INFO

Article history:
Received 24 May 2011
Received in revised form 9 July 2011
Accepted 12 July 2011
Available online 21 July 2011

Keywords:
SBA-15 silica spheres
Surface modification
Surface coverage
HPLC

ABSTRACT

Hexagonally ordered SBA-15 mesoporous silica spheres with large uniform pore diameters are obtained using the triblock copolymer, Pluronic P123, as template with a cosurfactant cetyltrimethylammonium bromide (CTAB) and the cosolvent ethanol in acidic media. A series of surface modified SBA-15 silica materials is prepared in the present work using mono- and trifunctional alkyl chains of various lengths which improves the hydrothermal and mechanical stability. Several techniques, such as element analysis, nitrogen sorption analysis, small angle X-ray diffraction, scanning electron microscopy (SEM), FTIR, solid-state ^{29}Si and ^{13}C NMR spectroscopy are employed to characterize the SBA-15 materials before and after surface modification with the organic components. Nitrogen sorption analysis is performed to calculate specific surface area, pore volume and pore size distribution. By surface modification with organic groups, the mesoporous SBA-15 silica spheres are potential materials for stationary phases in HPLC separation of small aromatic molecules and biomolecules. The HPLC performance of the present SBA-15 samples is therefore tested by means of a suitable test mixture.

1. Introduction

After the first report on surfactant templated synthesis of hexagonally ordered mesoporous MCM-41 silica materials in 1992, a broad spectrum of other mesoporous materials has been discovered. A major breakthrough in this area was the synthesis of large pore ordered mesoporous silica of the SBA-15 type using commercially available block copolymers. It is one of a series of mesoporous materials developed in the mid-late 1990s by Stucky et al. [1,2]. They reported that using triblock copolymers as structure directing agents, mesoporous silica can be synthesized in a wide range of sizes. Generally, the preparation includes the synthesis of a silica–surfactant composite, an aging step of the synthesis mixture under hydrothermal conditions, filtration with an optional washing step, followed by the removal of the organic polymer. The synthesis is based on a cooperative self-assembly of the silica precursor and micelles of the triblock copolymer as structure directing agents under acidic conditions. SBA-15 materials have hexagonal pore arrangement like MCM-41, with uniform pore diameters up to approximately 30 nm [2]. The pore diameters can be varied by changing the reaction condition. The specific surface areas and pore volumes of SBA-15 materials are somewhat smaller than those reported for the MCM-41 systems. At the same time, the SBA-15 materials are characterized by thicker pore walls which gives rise to an improved thermal and hydrothermal stability [3].

The morphology of SBA-15 can be well controlled by using block copolymers, cosurfactants or cosolvents [4], which makes such uniform materials useful for catalysis [5] and adsorption/desorption processes [6]. Application of large pore SBA-15 systems as a substrate in high performance liquid chromatography (HPLC) needs mono-disperse and micrometer-sized spherical particles.

In this contribution, we report the synthesis of well-ordered hexagonal SBA-15 mesoporous silica spheres with large uniform pore diameters. The synthesis was successfully conducted in strong acid media by using an amphiphilic block copolymer, poly(ethylene oxide)–poly(propylene oxide)–poly(ethylene oxide) and commercially available as Pluronic P123 ($EO_{20}PO_{70}EO_{20}$), as organic structure-directing agent in combination with a cosurfactant (CTAB) and ethanol as cosolvent.

It was reported earlier by Mesa et al. [7] that an adjustment of size and shape of the particles is only possible in the presence of the cosurfactant CTAB. In fact, it was observed that in the absence of a cosurfactant, the majority of the particles are very small with non-defined shape, indicating that the cosurfactant mainly determines the morphology of SBA-15 mesoporous silica. The cosolvent

* Corresponding author at: Institut für Physikalische Chemie, Universität Stuttgart, Pfaffenwaldring 55, D-70569 Stuttgart, Germany. Tel.: +49 711 6856 4469.
E-mail addresses: sci.yasmin@gmail.com, tahira.yasmin@ipc.uni-stuttgart.de (T. Yasmin).

0021-9673/$ – see front matter © 2011 Elsevier B.V. All rights reserved.
doi:10.1016/j.chroma.2011.07.035

ethanol also plays an important role for the formation of perfect spherical morphology. The addition of ethanol may decrease the polarity of the solvent, and thus decreases the rate of nucleation and growth of the mesostructure products because of the slower tetraethyl orthosilicate (TEOS) hydrolysis and mesostructure assembly, which contributes to the formation of silica spheres with smooth surfaces [8,9].

By surface modification with organic groups, mesoporous SBA-15 silica spheres can be used as a stationary phase in HPLC to separate both small aromatic molecules and biomolecules, such as proteins. Surface modification of the mesopore surfaces with, for instance, alkyl chains can be used to tailor the accessible pore sizes of the mesoporous solids, to increase surface hydrophobicity, to passivate remaining silanol groups, and thereby to protect the silica framework against hydrolysis. It is possible to progressively decrease the pore dimensions by the type (and length) of the employed alkyl chains. Recently, alkyl modified mesoporous SBA-15 silica materials were prepared and successively employed for the separation and analysis of inorganic ions, organic compounds and biological molecules [10].

Postsynthesis grafting techniques are commonly employed to attach organic groups to the silica surface. In this work, we report on the first systematic study of C_4 (*n*-butyl i.e., R = C_4H_9), C_8 (*n*-octyl i.e., R = C_8H_{17}), and C_{18} (*n*-octadecyl i.e., R = $C_{18}H_{37}$) modified SBA-15 materials which are prepared by chemical attachment of tri- or monofunctional silanes by means of the polymerization method. Surface modification takes place by forming Si–O–Si bonds due to the reaction between Si–OH (from SBA-15) and Si–OCH_3 groups (from the alkylsilanes). Si–O–Si bonds are also formed between adjacent Si–OCH_3 groups in the trifunctional chains. This makes the formation of monolayers with trifunctional silanes very attractive, since it provides closely packed and highly ordered monolayers with enhanced stability. However, the application of trifunctional silanes may also result in vertical polymerization [11] which may reduce the reproducibility in sample preparation. This undesired process can be avoided by surface modification using monofunctional silanes which provides reproducible surface coverages without vertical polymerization. For the SBA-15 materials modified with C_8 and C_{18} chains, a large fraction of non-reacted surface silanol group remains on the surface which is endcapped by reaction with hexamethyldisilazane (HDMS).

Several techniques such as element analysis, nitrogen sorption analysis, small angle X-ray diffraction, scanning electron microscopy (SEM), Fourier Transform infrared (FTIR), solid-state ^{29}Si and ^{13}C nuclear magnetic resonance (NMR) spectroscopy are employed to characterize the SBA-15 materials before and after surface modification with alkyl chains. Nitrogen sorption analysis is performed to calculate specific surface area, pore volume and pore size distribution (PSD). HPLC is employed to test the performance of surface modified SBA-15 silica materials as a stationary phase.

2. Experimental

2.1. Synthesis procedure

2.1.1. Chemicals

All materials were used as received without further purification, including Pluronic P123 (M_w = 5800, BASF), cetyltrimethylammonium bromide (CTAB, Aldrich), tetraethyl orthosilicate (TEOS, 98%, ACROS), hydrochloric acid (37%, Fluka), ethanol (100%, Fluka), the alkoxysilanes *n*-octadecyltrimethoxysilane, *n*-octadecyldimethylmethoxysilane, *n*-octyltrimethoxysilane, *n*-octyldimethylmethoxysilane, *n*-butyltrimethoxysilane and *n*-butyldimethylmethoxysilane (97%, Aldrich) and 1,1,1,3,3,3-hexamethyldisilazane (HMDS, 97%, Aldrich). Reagent grade toluene was distilled two times before use and was stored over molecular sieves.

2.1.2. Synthesis and surface modification of SBA-15 silica spheres

SBA-15 mesoporous silica spheres were synthesized using the triblock copolymer Pluronic P123 ($EO_{20}PO_{70}EO_{20}$) as a structure directing agent. 2 g of Pluronic P123 was dissolved by stirring in a solution of 10 ml of ethanol, 15 ml of water and 30 ml of 2 M HCl. Then 0.2 g of CTAB was added, followed by dropwise addition of 5 g of tetraethyl orthosilicate (TEOS). This mixture was stirred for 1 h, and was transferred to an autoclave for 5 h at 353 K. Loosely crosslinked SBA-15 particles precipitated during this reaction period at 353 K. The silica framework was further crosslinked by heating the reaction mixture for 15 h at 393 K. The as-synthesized SBA-15 material was filtered and dried overnight. After heating the sample at a rate of 1 K min^{-1}, the surfactant was removed by calcination in air at 823 K for 5 h.

Surface modification of the calcined SBA-15 silica material with mono- and trifunctional chains of different lengths (C_4, C_8 and C_{18}) was carried out by using the surface polymerization method. About 1 g sample of calcined SBA-15 silica was preevacuated at 378 K for 4 h and allowed to cool to ambient temperature. The resulting dry powder was equilibrated with humid air at room temperature for 6 h which gives a water layer on the silica surface [12,13]. Afterwards, humidified SBA-15 silica was suspended in 200 ml of toluene and heated to 343 K. The corresponding silane was first diluted in 50 ml of toluene, and the resulting solution was then added slowly to the SBA-15 suspension. This mixture was placed in a rotavapor for three days at 333 K.

From the SBA-15 materials surface modified with octyl (C_8) and octadecylsilanes (C_{18}), a fraction was used to endcap the remaining silanol groups with HMDS. The resulting SBA-15 silica spheres were filtered (G4 filter) and washed with toluene, followed by acetone, ethanol, ethanol/water (1:1, v:v.), water, ethanol, acetone, and pentane to rinse away any residual chemicals. The surface modified SBA-15 silica was dried overnight in an oven at 353 K and stored in airtight bottles.

2.2. Materials characterization

2.2.1. Elemental analysis

Carbon and hydrogen contents of all the surface modified SBA-15 silica materials were determined by a Carlo Erba Strumentazione elemental Analyzer 1106 (Milan, Italy). The percentage of carbon was utilized for calculating the surface coverage, α_{RP} (in $\mu mol\ m^{-2}$) on the basis of the following equation [14]:

$$\alpha_{RP} = \frac{10^6 P_C}{1200 n_C - P_C (M - n_x)} \frac{1}{S_{BET}}$$

where P_C the percentage of carbon determined via elemental analysis, n_C is the number of carbon atoms per silane moiety, M is the molar mass of the silane, n_x is the number of reactive groups in the silane (e.g., n_x = 3 for *n*-alkyltrimethoxysilane), and S_{BET} is the BET surface area of the unmodified support.

2.2.2. Nitrogen sorption studies

Nitrogen sorption (adsorption–desorption) measurements were performed at 77 K on a Micromeritics ASAP 2010 volumetric adsorption analyzer (Neuss, Germany). For the experiments, 150 mg of unmodified and all surface modified SBA-15 materials were degassed at 393 K for 4 h in the degassing port of the adsorption apparatus. The surface area measurements are based on the BET method within a pressure range from p/p_0 = 0.05–0.3. BET surface areas were calculated from the adsorption isotherms

using the BET equation [15] and a cross section for nitrogen $a(N_2) = 13.5$ Å^2 [16].

The pore volume was determined from the amount of N_2 adsorbed at a relative pressure of 0.99. The classical method of BJH cannot describe the sorption and phase behaviour of fluids in narrow mesopores (for widths < 100 Å) correctly, leading to an underestimation of the pore diameters [17]. Rather, a density functional theory (DFT) [18] based analysis appears as the most accurate method for pore size and pore size distribution determination. This approach takes into account the details of the fluid–fluid interactions and the adsorption potential, which depends on the strength of fluid wall interactions and the pore geometry. The DFT approach is based on a combination of statistical mechanical calculations and experimental observations for siliceous materials like macroporous silicas, zeolites, MCM-41 and SBA-15 silica materials [19–23]. The pore-filling pressures were determined as a function of the pore size from sorption isotherms on SBA-15 silica materials. The variation of the pore fluid density with pressure and pore size has been accounted for by DFT calculations. The DFT analysis was done with the DataMaster programme and the DFTplus module from Micromeritics.

2.2.3. Scanning electron microscopy

SEM measurements were performed on a CamScan CS44 scanning electron microscope (Waterbeach, UK). The samples were prepared by placing SBA-15 silica spheres on double-sided carbon adhesive tape mounted on the sample holder. The samples were then gold coated (thickness about 20 nm) by cathodic sputtering.

2.2.4. Small angle X-ray diffraction

X-ray diffraction experiments were performed with a Bruker AXS NanoSTAR system (CuK_α radiation aligned by Goebel mirrors) equipped with a two-dimensional electronic detector and a temperature controller (MRI Physikalische Geräte GmbH, Karlsruhe, Germany).

2.2.5. Solid-state NMR measurements

All ^{13}C and ^{29}Si NMR measurements were performed on a Varian InfinityPlus 400 NMR spectrometer (Varian, Palo Alto, CA, USA), operating at 9.4 T using a 4 mm MAS probe. Experiments were performed under magic angle spinning (MAS) conditions (sample rotation frequency: 5 kHz) at 100.52 MHz and 79.41 MHz, respectively. During the ^{13}C NMR experiments, cross-polarization (CP) excitation using $\pi/2$ pulse widths of 3.5 μs was employed. Contact time of 5 ms and recycle delays of 5 s were used. The typical number of scans was about 4000. The ^{13}C chemical shifts were determined relative to the external standard adamantane. ^{29}Si CP/MAS NMR spectra were recorded using a $\pi/2$ pulse length of 3.5 μs, a contact time of 5 ms, and a recycle delay of 5 s. The spinning speed was 5 kHz, and the typical number of scans was 5000. ^{29}Si chemical shifts were determined relative to external standard Q_8M_8, the trimethylsilylester of octameric silicate.

2.2.6. FTIR measurements

Pellets of surface modified SBA-15 materials and KBr (1/10 to 1/15, w/w) of 1 mm thickness were prepared under vacuum using a hydraulic press, and placed in a brass cell in a variable temperature transmission cell (L.O.T.—Oriel, Langenberg, Germany) equipped with NaCl windows. The spectra were recorded with a Nicolet Nexus 470 FTIR spectrometer (Nicolet, Madison, WI, USA) equipped with a DTGS detector, and by purging with N_2 gas. Typically, 256 interferograms, covering a spectral range of 4000–400 cm^{-1} at a resolution of 2 cm^{-1}, were collected within a temperature range from 193 K to 353 K. The recorded interferograms were apodized with a triangular function and Fourier transformed with two levels of zero filling. The background spectrum was recorded with the empty cell with twice the number of scans, as used for the measurements with the sample. Afterwards it was automatically subtracted from the subsequent spectra of surface modified SBA-15 silica materials. The processing and analysis of the spectra for CH_2 stretching band regions were performed with the OMNIC E.S.P.5.1 software (Nicolet). The wavenumbers of the CH_2 stretching vibrations were calculated from the interpolated zero crossing in the first derivative spectra.

2.2.7. HPLC experiments

Chromatographic columns (125 mm × 4.6 mm) were prepared for all the surface modified SBA-15 silica materials by the slurry method with acetone as solvent. The columns were packed using a Knauer pneumatic HPLC pump (Berlin, Germany) under 400 bar pressure in acetone. Chromatographic tests were performed at 25 °C using a Hewlett Packard HPLC instrument (Series 1100) from Agilent (Waldbronn, Germany) that possesses a UV–Visible diode array detector.

The chromatographic performance of these columns was tested with the reference mixture SRM 870 received from NIST, which contains five organic components: uracil, toluene, ethylbenzene, quinizarin, and amitriptyline. They were separated on the columns using an acetonitrile/water mixture (50/50, v/v) as mobile phase at an eluation velocity of 1.0 ml min^{-1} and with a detector operating at 254 nm. HPLC grade acetonitrile and water were obtained from Merck (Darmstadt, Germany).

3. Results and discussion

Well-ordered hexagonal SBA-15 mesoporous silica spheres were synthesized using commercially available block-copolymer surfactant in strong acid media. At first, a sample was prepared by heating the reaction mixture to 393 K for 20 h, from which, however, only irregular morphologies were obtained, as shown in Fig. 1(left). To get spherical particles, the reaction was divided into two steps. In the first step, the reaction mixture was heated at 353 K for 5 h. The resulting SBA-15 materials exhibit perfect spherical morphology, as shown in Fig. 1(middle), but the pore diameter and pore volume were found to be rather low. In a second step, the SBA-15 microspheres were therefore heated at 393 K for another 15 h. This second heating step at 393 K had no considerable effect on the morphology and size of the spheres (see Fig. 1, right), but a substantial increase in pore dimensions were observed for these SBA-15 materials, as will be further discussed below.

Alkyl groups (C_4, C_8 and C_{18}) were chemically attached to the calcined SBA-15 silica spheres by reaction with different silanes. The resulting materials are labelled as S-C*x*T or S-C*x*M, where *x* and M denote the alkyl chain length (*x* = 4, 8 and 18) and type of alkylsilane (T = trifunctional, M = monfunctional chains), respectively. Endcapped materials are labelled as S-C*x*TE or S-C*x*ME (see Table 1).

The percentage of carbon obtained from the elemental analysis of samples S-C18T and S-C18M are 12.92 and 1.67, respectively (see Table 2). The respective surface coverage calculated for the material modified with the monofunctional silane is relatively low (0.11 μmol m^{-2}) which is a direct result of the presence of only one reactive methoxy group. It is seen that surface modification with the monofunctional silane yields only moderate surface coverages since further cross-linking of the silanes is not possible. The trifunctional silane gives much higher surface coverage (1.05 μmol m^{-2}), because the trifunctional chains can directly bind to the surface silanol groups, and are able to undergo cross-linking reactions with neighbouring silane chains. Hence, the latter assemblies typically exhibit a better chain packing with higher surface coverage, good thermal and enhanced chemical stability. Similar trends are

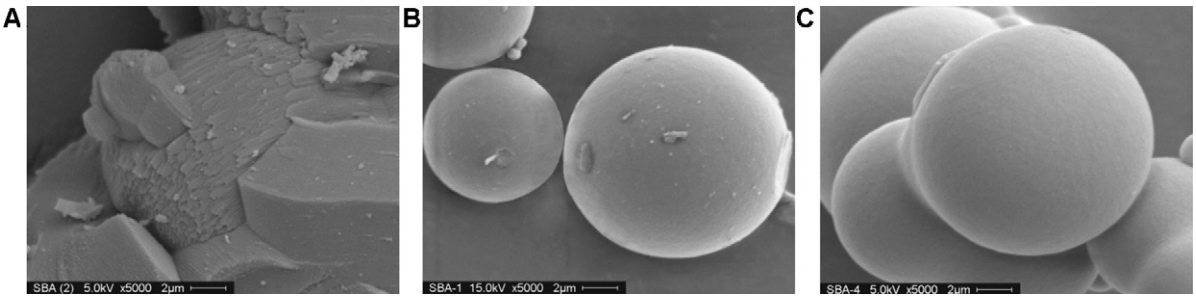

Fig. 1. SEM micrographs for SBA-15 materials prepared by directly heating to 393 K (A), prepared at 353 K (B) and prepared at 353 K followed by second heating step at 393 K (C).

Table 1
Surface modified SBA-15 silica materials and their material codes.

Material code	Surface modified SBA-15 silica materials
S-C4T	SBA-15 modified with *n*-butyltrimethoxysilane
S-C8T	SBA-15 modified with *n*-octyltrimethoxysilane
S-C8TE	SBA-15 modified with *n*-octyltrimethoxysilane and endcapped with HMDS
S-C18T	SBA-15 modified with *n*-octadecyltrimethoxysilane
S-C18TE	SBA-15 modified with *n*-octadecyltrimethoxysilane and endcapped with HMDS
S-C4M	SBA-15 modified with *n*-butyldimethylmethoxysilane
S-C8M	SBA-15 modified with *n*-octyldimethylmethoxysilane
S-C8ME	SBA-15 modified with *n*-octyldimethylmethoxysilane and endcapped with HMDS
S-C18M	SBA-15 modified with *n*-octadecyldimethylmethoxysilane
S-C18ME	SBA-15 modified with *n*-octadecyldimethylmethoxysilane and endcapped with HMDS

observed for the SBA-15 systems modified with the shorter C4 and C8 chains, samples S-C8T, S-C8M, S-C4T, and S-C4M (see Table 2).

The derived data for the surface coverage clearly also demonstrate a higher surface coverage for the samples modified with shorter alkyl chains which can be explained by the possibility and enhanced probability for the shorter chains to bind at the interior of the mesoporous channels. The longer chains are assumed to bind primarily on the surface of the SBA-15 materials, and – due to sterical hindrance – have less chance to advance to the interior part of the channels. Therefore, endcapping with HMDS was carried out for the SBA-15 materials surface modified with C_8 and C_{18} alkyl chains. As can be seen from the data in Table 2, endcapping shows for all samples the expected increase of the carbon content and surface coverage.

SEM pictures of the spheres of mesoporous SBA-15 materials are shown in Fig. 1. As mentioned above, the SBA-15 sample, obtained by directly heating the reaction mixture to 393 K, exhibits irregular morphology (Fig. 1A), while the spherical morphology of the SBA-15 samples prepared at 353 K and by the two-step procedure is clearly visible in Fig. 1 B and C, respectively.

Nitrogen sorption isotherms of the SBA-15 samples are used to obtain information about the mesoporosity. Table 2 lists all derived nitrogen sorption parameters. Nitrogen sorption isotherms are given in Fig. 2(top), while DFT pore size distributions for unmodified SBA-15 and the materials after surface modification with trifunctional alkylsilanes are shown in Fig. 2(bottom). Fig. 3 shows nitrogen sorption isotherms and DFT pore size distributions for the SBA-15 samples treated with monofunctional chains.

The nitrogen sorption isotherms are characterized by a typical irreversible IV type isotherm with a H1 hysteresis loop [24]. They exhibit a sharp inflection in the p/p_0 range from 0.60 to 0.80, characteristic of capillary condensation within uniform pores. The p/p_0 positions of the inflection points are related to the diameter in the mesopore range, and the sharpness of the step indicates the uniformity of the mesopore size distribution. The overall appearance of the nitrogen sorption isotherms of the surface modified SBA-15 samples is similar to that of the unmodified SBA-15 material. In general, there is a notable shift of the hysteresis position towards lower p/p_0 values along with a decrease in overall nitrogen adsorption volume with increasing surface coverage. The SBA-15 samples which are surface modified with the trifunctional alkylsilanes exhibit a stronger reduction in surface area, pore diameter and total pore volume than those from modification with monofunctional silanes. The reduction in these surface parameters is larger for the C_4 and C_{18} chains than for the samples surface modified with C_8 chains. The reason for this is that the shorter C_4 chains have greater ability to incorporate in the channels of the SBA-15 material as compared

Table 2
Nitrogen sorption parameters for SBA-15 materials before and after surface modification.

Material code	S_{BET} (m^2/g)	V_p (ml/g)	DFT D_{pore} (nm)	% C	SC (μmol/m^2)
SBA-15	735	1.52	10.10	–	–
S-C4T	484	0.88	9.01	6.61	3.75
S-C8T	501	0.89	9.15	9.42	1.73
S-C8TE	428	0.83	8.28	10.60	2.02
S-C18T	380	0.76	8.70	12.92	1.05
S-C18TE	308	0.60	8.28	18.43	1.70
S-C4M	532	1.02	9.35	5.50	2.58
S-C8M	560	1.16	9.64	2.90	0.57
S-C8ME	450	0.91	8.71	8.57	1.48
S-C18M	532	1.13	9.63	1.67	0.11
S-C18ME	378	0.80	9.14	9.40	0.70

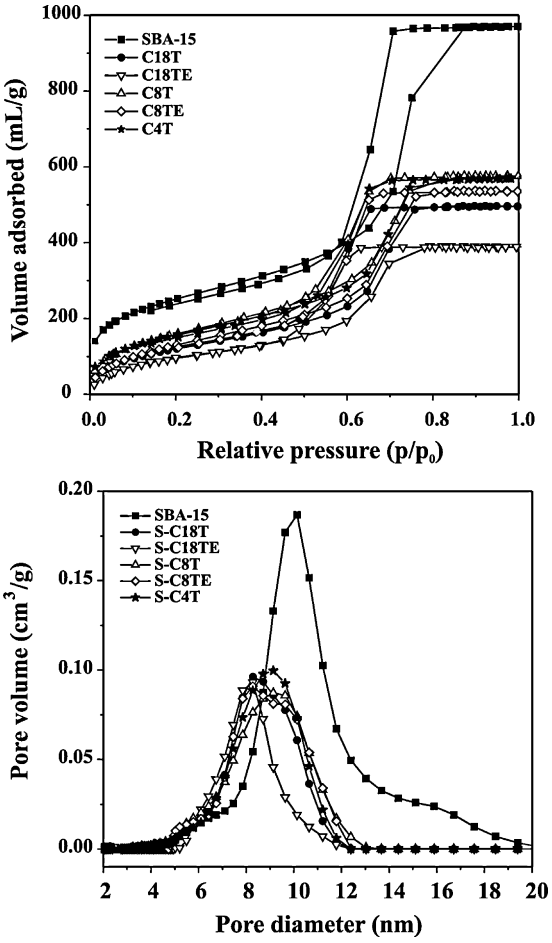

Fig. 2. Nitrogen sorption isotherms (top) and DFT pore size distributions (bottom) for SBA-15 materials before and after surface modification with trifunctional alkylsilanes.

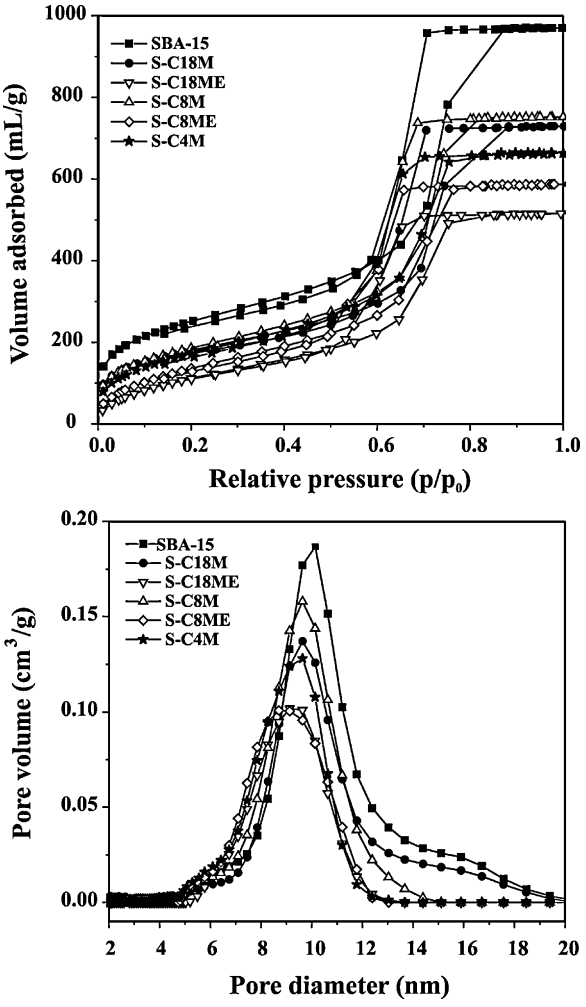

Fig. 3. Nitrogen sorption isotherms (top) and DFT pore size distributions (bottom) for SBA-15 materials before and after surface modification with monofunctional alkylsilanes.

to the longer chains and longer C_{18} chains have ability to cover the surface as compared to the shorter chains.

Fig. 4 depicts the XRD pattern obtained for calcined SBA-15 and surface modified SBA-15 samples. All of them show a single diffraction peak, characteristic of mesoporous materials with a pore structure with a lack of long-range order. Surface modification does not affect the XRD pattern, indicating that the hexagonal symmetry and the inorganic wall structure of the SBA-15 material is retained.

^{29}Si NMR spectroscopy was employed for the determination of the surface species, amount of alkyl chain attachment and degree of cross-linking of the attached alkylsilanes. The ^{29}Si CP/MAS NMR spectra of the unmodified and surface modified SBA-15 samples are shown in Fig. 5, and the chemical shifts are reported in Table 3. The ^{29}Si resonances around −92, −102 and −110 ppm originate from the structural units of the SBA-15 support and reflect surface silanol groups, Q^2, Q^3 and Q^4 groups, respectively (Q^n units = $Si(OSi)_n(OH)_{4-n}$, with n = 1–4) [14,25]. After attachment of the butyl, octyl and octadecyl chains, the intensities of Q^2 and Q^3 units, bearing surface hydroxyl groups, are significantly reduced, while the relative intensity for the Q^4 units increases. The same trend can be also seen for the endcapped samples.

The Q^2 groups are lost in case of materials surface modified with shorter trifunctional chains (C_4 and C_8) owing to their greater reactivity. The Q^3 signal intensity for the samples modified with monofunctional alkylsilanes is found to be higher than for those obtained from trifunctional alkylsilanes, which is consistent with the lower surface coverage. This can be related to the lower reactivity of the former silylation reagent due to the lower probability (only one reactive group available) to react with surface silanols. Further reasons might be the bulky methyl groups of the monofunctional alkylsilane, which provide a steric hindrance for the binding of other alkylsilane chains in close vicinity to a surface-bound alkylsilane.

For the endcapped materials, an additional peak at about 13 ppm [M = $R_3Si(OSi–)$] is found arising from the trimethylsilyl groups of the endcapping reagent. For sample, S-C8ME and S-C18ME samples, this peak also contains a small signal component from the attached monofunctional alkylsilane chains of the first surface modification step. This latter peak has very low intensity in the case of material modified with C_{18} monofunctional chain (S-C18M) because only a small amount of C_{18} monofunctional chains is bound to the SBA-15 surface, as also reflected by the very low surface coverage.

In the case of materials surface modified with trifunctional chains, the presence of T^1, T^2 and T^3 peaks (at about −49 ppm, −56 ppm and −65 ppm) prove the attachment and cross-linking of the chains on the SBA-15 silica surface ($T^n = RSi(OSi)_n(OH)_{3-n}$, with n = 1, 2, 3) [26]. T^1 signals denote trifunctional groups without cross-linking, while T^2 and T^3 signals arise from groups with partial and complete cross-linking, respectively. The intensity of these T peaks is found to increase with the increasing surface coverage of the materials which is in line with an increase in the degree of cross-linking. The highest intensity of these peaks is observed

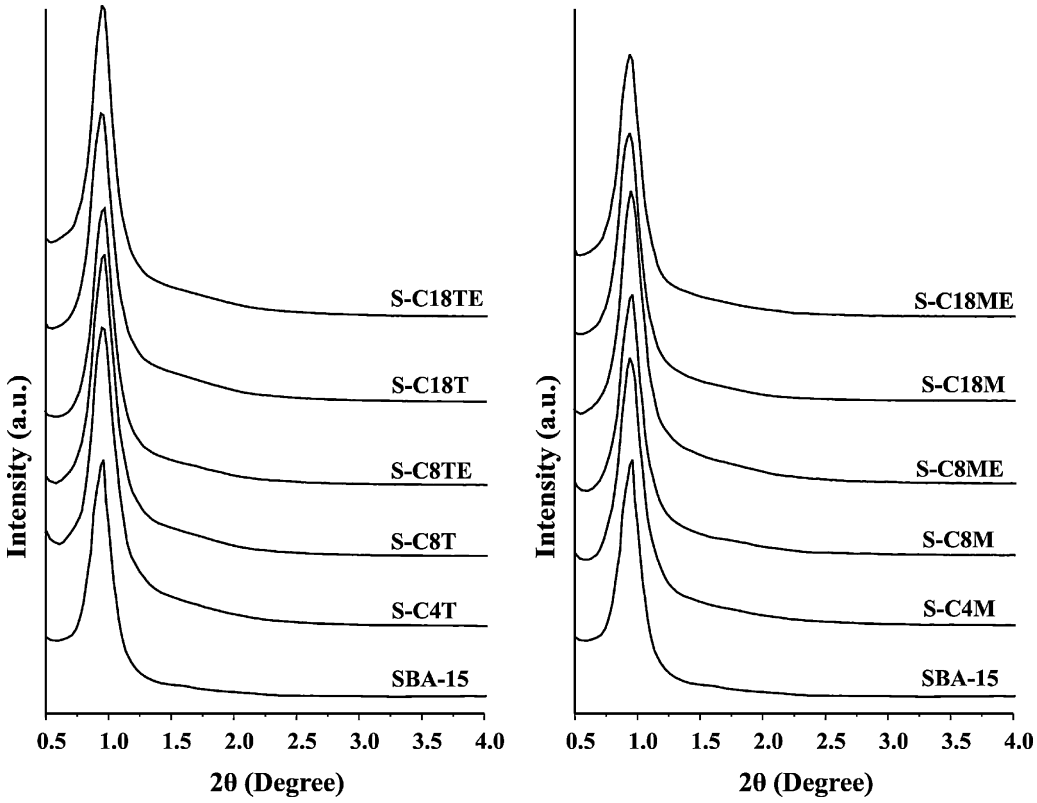

Fig. 4. XRD patterns for SBA-15 materials before and after surface modification with trifunctional alkylsilanes (left) and monofunctional alkylsilanes (right).

for the sample from modification with C_4 trifunctional chains, in agreement with the higher surface coverage of this material.

^{13}C NMR spectroscopy was used to study the organic components after attaching alkyl chains to the SBA-15 silica surface. The experimental ^{13}C CP/MAS NMR spectra for the surface modified SBA-15 silica materials are given in Fig. 6. The ^{13}C chemical shifts of the various species are reported in Table 4. The SBA-15 samples surface modified with octadecylsilanes show the typical NMR resonances for aliphatic carbons [27].

The ^{13}C NMR spectra of the SBA-15 materials surface modified with octadecylsilanes are dominated by the signal from the internal carbons (C3–C16) at about 30 ppm. It is well known that ^{13}C chemical shifts of the methylene carbons located in the inner part of alkyl chain are very sensitive to the conformational states [28–30]. The methylene carbons in all-trans conformation have a chemical shift between 34.2 ppm and 32.8 ppm depending on their molecular packing and motional state, while the chemical shift of those in a mixed trans-gauche conformation is up-field shifted [28,30,31]. The maximum shift difference of methylene carbons due to these different conformational states was reported as ~5 ppm [32]. The chemical shift value of the C3–C16 peak of about 30 ppm, observed for the octadecyl chains bound to the SBA-15 surface, implies that the carbons are in a mixed trans-gauche conformation. The SBA-15 samples treated with trifunctional alkylsilanes exhibit a resonance at about 50 ppm which cannot be assigned to the carbon atoms of the surface bound octadecyl silane molecules, unless some non-reacted methoxy groups are still present. Another, more likely explanation are methoxy groups which were released during the hydrolysis of the trifunctional silanes, and which are subsequently bound to the surface silanol groups [33]. For the SBA-15 sample surface modified with monofunctional octadecylsilane (S-C18M), the methyl groups bound to the silicon atom of the alkylsilane resonate at about −1.8 ppm.

The resonances for the SBA-15 samples surface modified with mono- and trifunctional octylsilanes and butylsilanes (see Table 4) were assigned according to literature [34,35]. Again, for the samples treated with trifunctional alkylsilanes, an additional ^{13}C resonance at around 50 ppm is observed which either stems from the

Table 3
^{29}Si CP/MAS chemical shift values for SBA-15 materials before and after surface modification.

Material code	^{29}Si chemical shift (ppm)						
	Q^2	Q^3	Q^4	T^1	T^2	T^3	M
SBA-15	−92.3	−101.1	−111.0	–	–	–	–
S-C4T	–	−101.5	−109.7	−48.8	−56.3	−64.8	–
S-C8T	–	−101.6	−109.9	−48.7	−56.2	−65.7	–
S-C8TE	–	−101.1	−109.0	−49.8	−56.0	−65.5	13.3
S-C18T	−92.4	−101.8	−110.3	−48.7	−56.2	–	–
S-C18TE	–	−102.0	−109.2	−49.9	−56.1	−65.3	13.2
S-C4M	−92.4	−101.8	−110.7	–	–	–	13.7
S-C8M	−92.2	−101.6	−110.7	–	–	–	12.9
S-C8ME	–	−101.7	−109.3	–	–	–	12.8
S-C18M	−92.7	−101.7	−111.3	–	–	–	13.2
S-C18ME	–	−102.3	−109.6	–	–	–	12.6

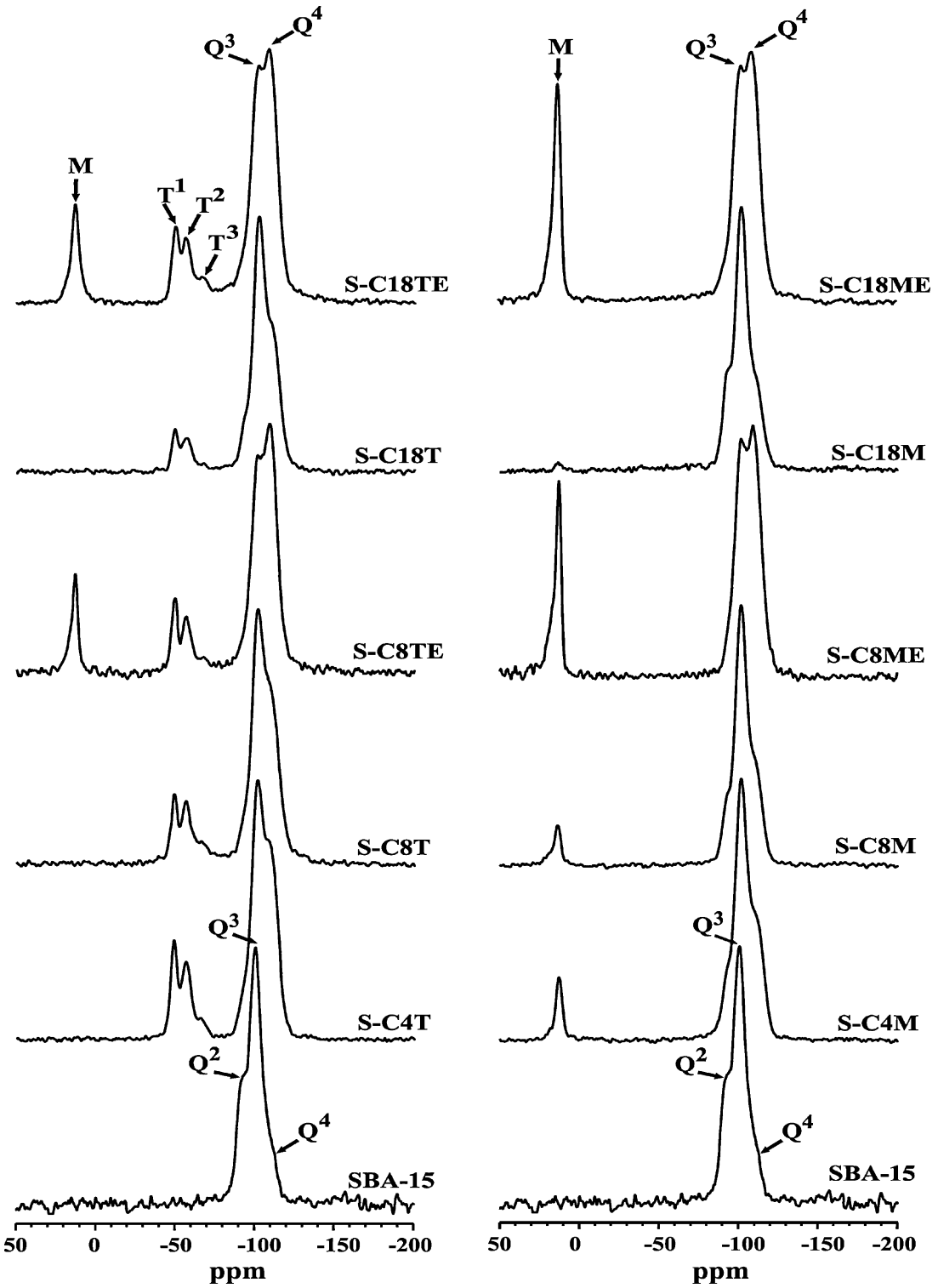

Fig. 5. ^{29}Si CP/MAS NMR spectra of SBA-15 materials before and after surface modification with trifunctional alkylsilanes (left) and monofunctional alkylsilanes (right).

nonreacted methoxy groups or methoxy groups bound to the silica surface (see above).

The trimethylsilyl groups after endcapping with HMDS resonate at 0.1 ppm and 0.4 ppm for samples S-C8TE and S-C18TE, respectively. For the samples S-C8ME and S-C18ME, this signal appears at 0.2 ppm and 0.5 ppm, respectively. In the latter case, the signal also contains a spectral component from the methyl groups of the attached dimethylalkyl silane which due to the residual NMR linewidth cannot be separated from HMDS resonance.

FTIR spectroscopy can be used to probe the structural features of the attached alkyl chains. In general, the conformational properties of attached alkyl chains can be studied by several conformation-sensitive vibrational bands [36,37]. Among these, the symmetric and antisymmetric CH_2 stretching bands (2800–3000 cm^{-1}) are the most intense signals, and in the majority of cases are easily accessible. Their positions as a function of external parameters, like temperature, pressure or sample constitution, can be used for a qualitative discussion of the conformational order in the aliphatic

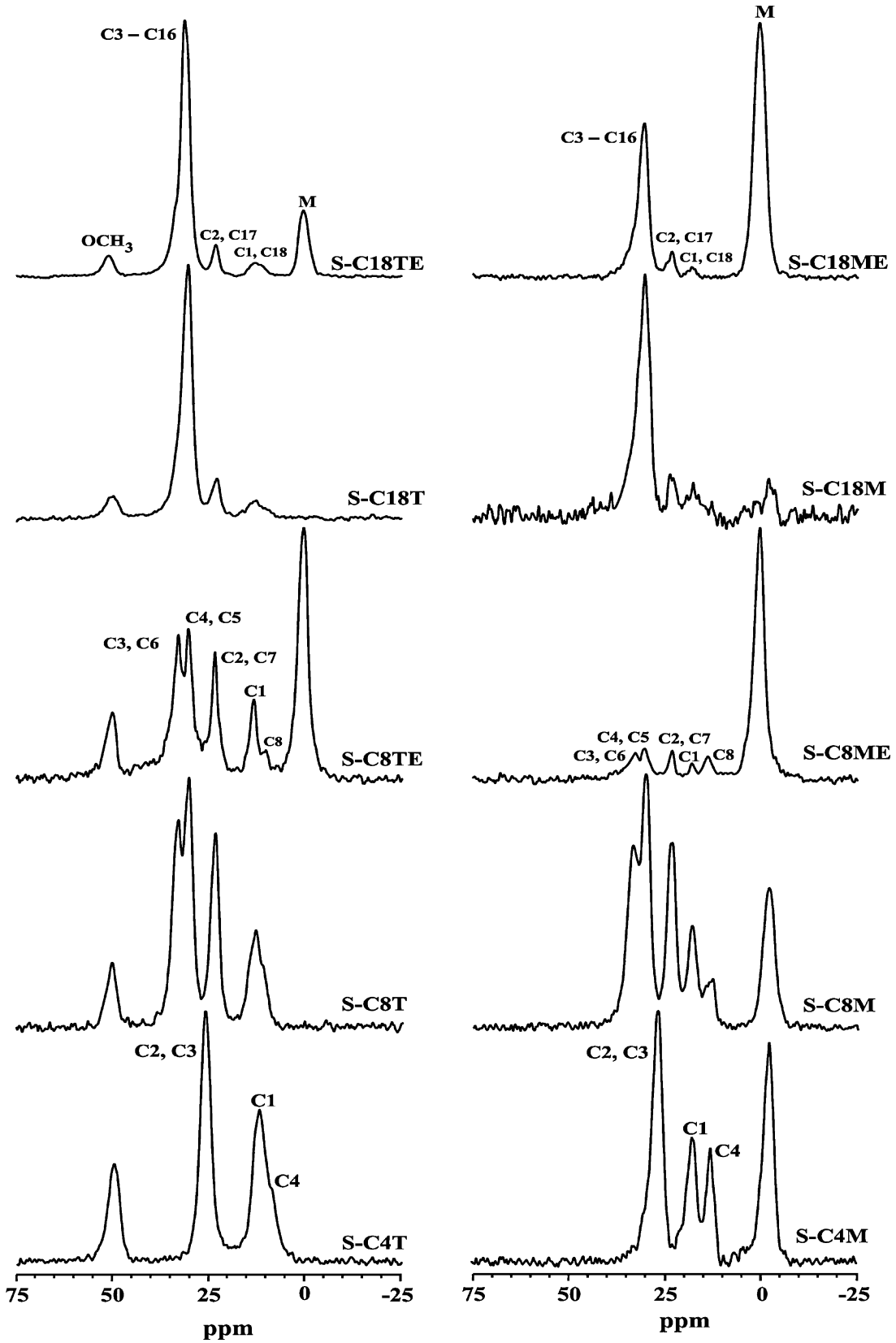

Fig. 6. ^{13}C CP/MAS NMR spectra of SBA-15 materials before and after surface modification with trifunctional alkylsilanes (left) and monofunctional alkylsilanes (right).

chains. Hence, changes in the positions of these bands are directly related to the alteration of the *trans*/*gauche* ratios. A band shift towards lower wavenumbers reflects an increase in conformational order (i.e., higher amount of *trans* conformers and reduced mobility), while a shift towards higher wavenumbers points to an increasing conformational disorder with a higher amount of *gauche* conformers, and thus enhanced chain flexibility. Similar information can, in principle, be derived from the bandwidths, although

Table 4
^{13}C chemical shifts and assignment of surface modified SBA-15 materials.

Sample	Carbon position	^{13}C shift (ppm)	Sample	Carbon position	^{13}C shift (ppm)
S-C4T	OCH_3	49.6	S-C4M	$Si(CH_3)_2$ R	−2.2
	C-4	10.2		C-4	12.9
	C-1	12.1		C-1	17.7
	C-2, C-3	25.9		C-2, C-3	26.4
S-C8T	OCH_3	50.3	S-C8M	$Si(CH_3)_2$ R	−2.0
	C-8	10.7		C-8	12.7
	C-1	12.8		C-1	18.0
	C-2, C-7	23.3		C-2, C-7	23.2
	C-4, C-5	30.2		C-4, C-5	30.1
	C-3, C-6	32.9		C-3, C-6	32.7
S-C8TE	OCH_3	49.9	S-C8ME	$Si(CH_3)_2$ R, $Si(CH_3)_3$	0.2
	$Si(CH_3)_3$	0.1		C-8	13.5
	C-8	13.2		C-1	18.6
	C-1	17.4		C-2, C-7	23.4
	C-2, C-7	23.3		C-4, C-5	30.5
	C-4, C-5	30.2		C-3, C-6	33.5
	C-3, C-6	32.9			
S-C18T	OCH_3	50.1	S-C18M	$Si(CH_3)_2$ R	−1.8
	C-1, C-18	12.6		C-1, C-18	16.8
	C-2, C-17	22.8		C-2, C-17	23.6
	C-3–C-16	30.4		C-3–C-16	30.2
S-C18TE	OCH_3	50.7	S-C18ME	$Si(CH_3)_2$ R, $Si(CH_3)_3$	0.5
	$Si(CH_3)_3$	0.4		C-1, C-18	16.9
	C-1, C-18	13.1		C-2, C-17	23.3
	C-2, C-17	23.5		C-3–C-16	30.4
	C-3–C-16	31.3			

the respective bandwidth alterations are typically less pronounced [38].

Variable temperature FTIR studies were performed for the present surface modified SBA-15 materials in a temperature range between 193 K and 353 K. Representative FTIR spectra, covering the region of the CH_2 and CH_3 stretching bands, are shown in Figs. 7 and 8, and all spectra for both endcapped and non-endcapped materials are shown in the Supplementary materials section. Information about the alkyl chain conformational order (along with its temperature dependence) is important in connection with the chromatographic separations, where the shape selectivity can be affected by column temperature and thus conformation features of the stationary phase.

The bands are assigned according to previous studies [39–44]. The CH_3 groups exhibit antisymmetric (CH_3-a) and symmetric (CH_3-s) stretching modes near 2962 cm^{-1} and 2872 cm^{-1} while for the CH_2 groups these modes occur near 2927 cm^{-1} (CH_2-a) and 2857 cm^{-1} (CH_2-s), respectively. For sample S-C4T (see Fig. 7) the symmetric CH_2 band is split into two bands at 2866 cm^{-1} and 2852 cm^{-1} at 193 K. According to Fox and Martin [41,45], this split can arise from coupling between the 2 methylene units. A similar split-up of this IR band has been also reported for alkyl bonded silica systems [46–48]. At higher temperatures, the bands broaden, and the splitting becomes successively smaller showing an increasing conformational disorder with increasing temperature.

For the sample S-C8T, at 193 K the antisymmteric and symmetric CH_2 stretching bands are visible at 2929 cm^{-1} and 2857 cm^{-1}, respectively. Upon temperature increase, these bands are slightly shifted towards higher wavenumbers to reach values of 2930 cm^{-1} and 2858 cm^{-1}, respectively, at 353 K. For the sample S-C8TE, the antisymmteric and symmetric CH_2 stretching bands appear at 2929 cm^{-1} and 2856 cm^{-1} and are showing a wavenumber shift of 2 cm^{-1} towards higher values at higher temperatures. Such shifts for the CH_2 stretching bands are well documented for many materials [14,38,49].

In the case of S-C18T sample, at 193 K 2 bands appear at 2925 cm^{-1} for antisymmteric CH_2 stretching band and 2854 cm^{-1} for symmetric CH_2 stretching band. These bands are found to shift towards higher wavenumbers with increasing sample temperature and are shifted to 2927 cm^{-1} and 2856 cm^{-1}, respectively at 353 K. For the sample S-C18TE, these bands are shifted from 2924 cm^{-1} and 2854 cm^{-1} to 2927 cm^{-1} and 2857 cm^{-1}. Here we observe a higher frequency shift of almost 3 cm^{-1} pointing to an increasing conformational disorder with a higher amount of the gauche conformers and thus higher alkyl chain mobility [50].

Fig. 8 shows the FTIR spectra of SBA-15 materials surface modified with monofunctional chains. Here, two methyl groups are bound to the silicon atom in the alkyl chains which explains the higher relative intensity of the antisymmetric CH_3 stretching bands. For the sample S-C4M, there is no split-up of the symmetric CH_2 band, as observed for sample S-C4T. In the sample S-C8M, the antisymmteric CH_2 stretching band appears at 2926 cm^{-1} and shifting to 2928 cm^{-1}. While the symmetric CH_2 stretching band appears at 2857 cm^{-1} and shifting to 2858 cm^{-1}. In the sample S-C8ME, the antisymmteric and symmetric CH_2 stretching bands are showing an increase of 2 cm^{-1} upon temperature increase. For samples surface modified with the monofunctional octyl chains, the CH_2 stretching bands appear at lower wavenumbers owing to the lower conformational order of the monofunctional octyl chains as compared to the trifunctinal ones.

In the sample S-C18M, the antisymmteric and symmetric CH_2 stretching bands appear at 2927 cm^{-1} and 2855 cm^{-1} and are shifting to 2928 cm^{-1} and 2856 cm^{-1}, respectively. For the sample S-C18ME, there is a shift of 2 cm^{-1} in wavenumber as the temperature is increasing. The CH_2 stretching bands appear at higher wavenumbers in materials surface modified with the monofunctional octadecyl chains as compared to corresponding trifunctional materials. This implies that the conformational order in the samples surface modified with monofunctional octadecyl chains is higher than in the trifunctional materials despite the higher carbon content (and thus higher surface coverage) of the latter SBA-15 materials. A possible explanation might be given by the stronger intermolecular interactions of the methyl groups bound to the silicon atom for the monofunctional samples, comprising chain–chain

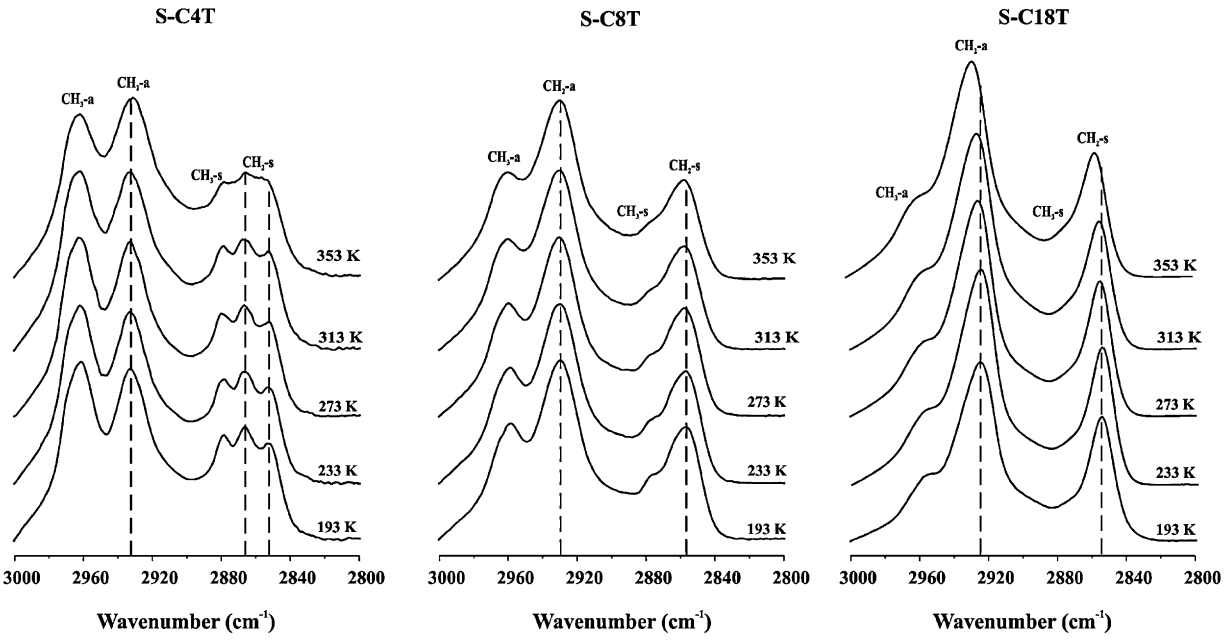

Fig. 7. Representative variable temperature FTIR spectra of SBA-15 materials surface modified with trifunctional alkylsilanes.

as well as chain–silica surface interactions, and which imposes a higher chain order than for the trifunctional samples.

3.1. HPLC measurements

The chromatographic performance of surface modified SBA-15 silica spheres was tested using a test mixture, NIST SRM 870, which consists of 5 organic components (uracil, toluene, ethylbenzene, quinizarin and amitriptyline) under controlled conditions, i.e., mobile phase, flow, and temperature.

Fig. 9 shows the separation chromatograms of the aforementioned test mixture by using the surface modified SBA-15 silica columns with a mobile phase of acetonitrile/water – 50/50 (v/v) at a flow rate of 1.0 ml min^{-1}. The eluent time of organic components under these separation conditions follows the order: uracil < toluene < ethylbenzene < quinizarin < amitriptyline. As expected, for reversed-phase chromatography, the more polar compounds elute faster than the less polar molecules. This can be understood by the greater affinity of the polar molecules towards the polar mobile phase. Hence, the less polar or non-polar molecules will elute much slower because of their interaction with non-polar stationary phase.

In the majority of the cases, well-separated peaks for uracil, toluene, ethylbenzene, quinizarin, and amitriptyline can be observed. Surface coverage and alkyl chain lengths are the main factors which affect the chromatographic performance of the stationary phases. Therefore, the test mixture is well separated with good peak shapes for the stationary phases with higher surface coverage for the alkylsilanes. The materials with lower surface coverages possess residual silanol groups which is mainly observed

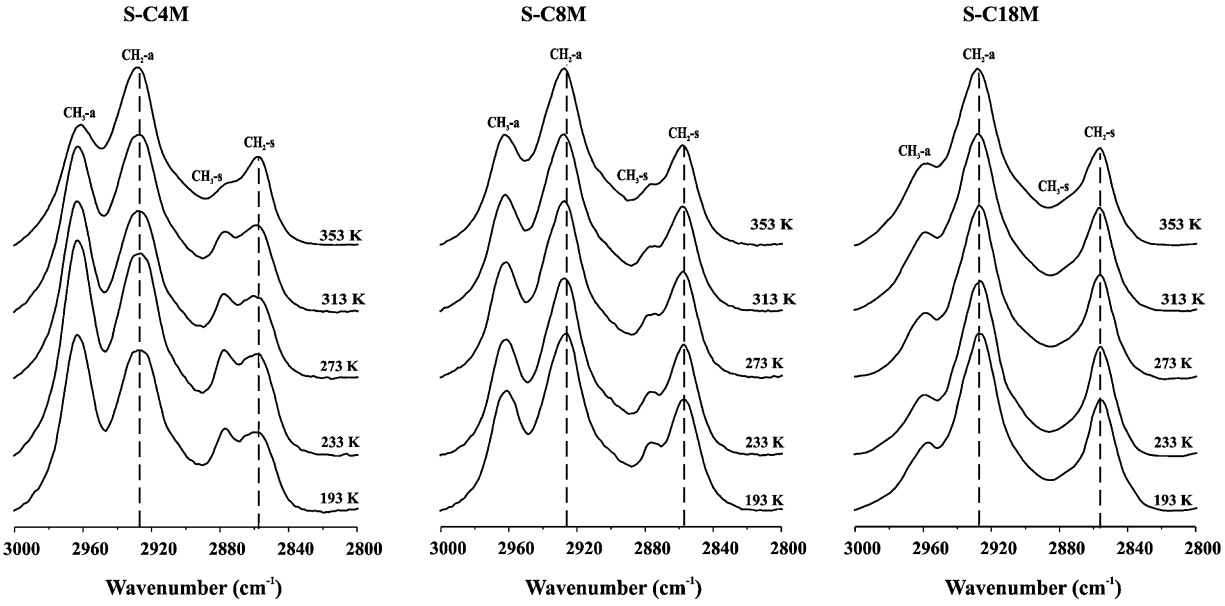

Fig. 8. Representative variable temperature FTIR spectra of SBA-15 materials surface modified with monofunctional alkylsilanes.

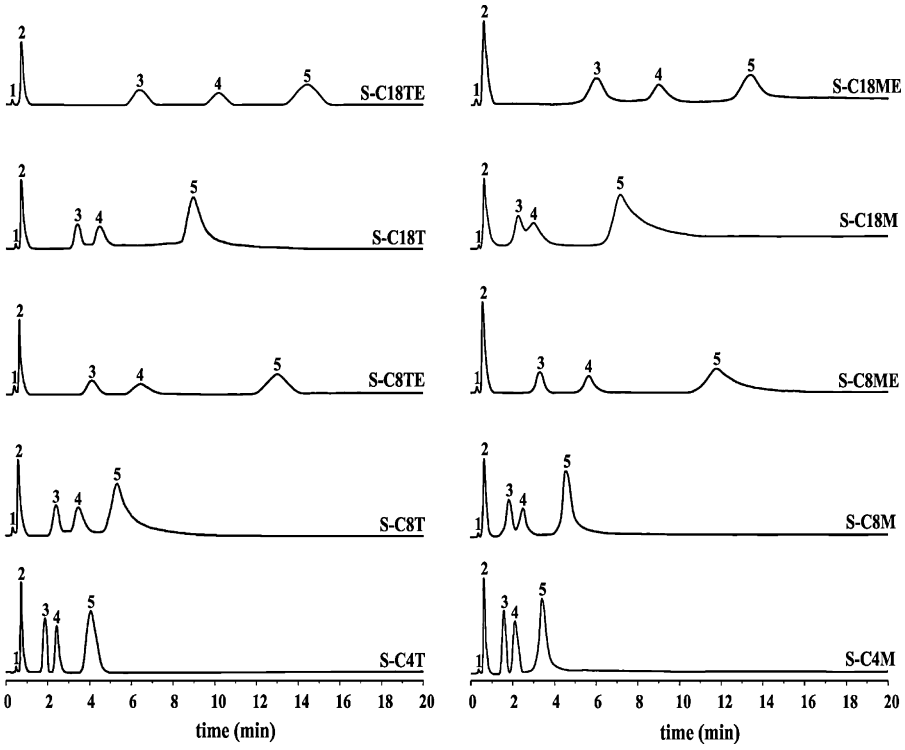

Fig. 9. HPLC diagrams for test mixture SRM 870 mixture: uracil (1), toluene (2), ethylbenzene (3), quinizarin (4) and amitriptyline (5) using a acetonitrile/water mixture (50/50, v/v) as the mobile phase at flow rate of 1.0 ml min^{-1} at 254 nm for SBA-15 materials before and after surface modification.

for materials modified with longer alkyl chains, C_8 and C_{18}, where the longer chains are mostly bound to the outer surface and only a few chains are attached within the mesopores due to steric hindrance. The remaining silanol groups are weakly acidic, and cause peak tailing of basic solutes (in samples S-C8T, S-C8M, S-C18T and S-C18M), which reduces resolution and column efficiency in chromatographic separations. Endcapping of these remaining silanols significantly improves the peak shapes and the chromatographic performance because at higher surface coverages, only a small number of silanols remains, and symmetric peak shapes are observed [51]. However, like the observations for longer alkylsilane chains, the increasing hydrophobicity of the surface, in general, also increases the eluation time.

4. Concluding remarks

Mesoporous SBA-15 silica spheres were prepared using a triblock copolymer, and their spherical morphology was confirmed by SEM analysis. SBA-15 materials with desired surface properties were prepared by surface modification using mono- and trifunctional alkylsilane chains with different lengths. The mesoporosity and hexagonal pore symmetry of the material is retained after surface modification which was confirmed by nitrogen sorption and XRD studies. Alkyl chain attachment and chain cross-linking were studied by ^{29}Si and ^{13}C NMR spectroscopies. FTIR and ^{13}C NMR measurements revealed a low conformational order of the alkyl chains for the materials surface modified with monofunctional alkylsilanes as compared to materials modified with trifunctional alkylsilanes which can be understood by the higher surface coverage, alkylchain packing and stronger chain–chain interactions of the latter ones. For the alkylsilanes with shorter chain lengths higher surface coverages were found, as they can also bind to the interior of the mesopores. The chromatographic performance was tested, and surface coverage and alkyl chain length are the main factors that affect the chromatographic performance. A better separation performance was found for the SBA-15 silica materials with higher surface coverage. A further improvement of the chromatographic separation for the SBA-15 samples surface modified with longer alkyl chains was achieved by subsequent endcapping with HMDS. In summary, these mesoporous SBA-15 silica are suitable stationary phase materials for chromatographic applications, and the choice of alkylsilane for surface modification is based upon the solubility and polarity of the test analytes.

Acknowledgments

The authors would like to thank Professor Dr. E. Roduner (Institute of Physical Chemistry, University of Stuttgart) for access to the nitrogen sorption instrument, Dr. A. Fels (Institute of Electron microscopy microanalyses, University of Stuttgart) for the SEM measurements and analysis, Professor Dr. F. Giesselmann and Ms. N. Kapernaum (Institute of Physical Chemistry, University of Stuttgart) for their assistance during XRD measurements, and Dr. Dirnberger (Institute of Polymer Chemistry, University of Stuttgart) for support during the HPLC experiments. Higher Education Commission (HEC), Pakistan and DAAD are greatly acknowledged for a doctoral fellowship.

Appendix A. Supplementary data

Supplementary data associated with this article can be found, in the online version, at doi:10.1016/j.chroma.2011.07.035.

References

[1] D.Y. Zhao, Q.S. Huo, J.L. Feng, B.F. Chmelka, G.D. Stucky, J. Am. Chem. Soc. 120 (1998) 6024.
[2] D.Y. Zhao, J.L. Feng, Q.S. Huo, N. Melosh, G.H. Fredrickson, B.F. Chmelka, G.D. Stucky, Science 279 (1998) 548.
[3] A. Vinu, M. Hartmann, Chem. Lett. 33 (2004) 588.
[4] D.Y. Zhao, J.Y. Sun, Q.Z. Li, G.D. Stucky, Chem. Mater. 12 (2000) 275.

[5] A. Galarneau, D. Desplantier-Giscard, F. Di Renzo, F. Fajula, Catal. Today 68 (2001) 191.
[6] A.M. Liu, K. Hidajat, S. Kawi, D.Y. Zhao, Chem. Commun. (2000) 1145.
[7] M. Mesa, L. Sierra, B. Lopez, A. Ramirez, J.L. Guth, Solid State Sci. 5 (2003) 1303.
[8] K. Kosuge, P.S. Singh, Chem. Mater. 13 (2001) 2476.
[9] Y.R. Ma, L.M. Qi, J.M. Ma, Y.Q. Wu, O. Liu, H.M. Cheng, Colloids, Surf. A-Physicochem. Eng. Aspects 229 (2003) 1.
[10] J.W. Zhao, F. Gao, Y.L. Fu, W. Jin, P.Y. Yang, D.Y. Zhao, Chem. Commun. (2002) 752.
[11] C.P. Tripp, M.L. Hair, Langmuir 11 (1995) 1215.
[12] M.J. Wirth, H.O. Fatunmbi, Anal. Chem. 65 (1993) 822.
[13] L.C. Sander, S.A. Wise, Anal. Chem. 67 (1995) 3284.
[14] S. Singh, J. Wegmann, K. Albert, K. Müller, J. Phys. Chem. B 106 (2002) 878.
[15] S. Brunauer, P.H. Emmett, E. Teller, J. Am. Chem. Soc. 60 (1938) 309.
[16] L. Jelinek, E.S. Kovats, Langmuir 10 (1994) 4225.
[17] Y. Zhang, F.L.Y. Lam, Z.F. Yan, X.J. Hu, Chin. J. Chem. Phys. 19 (2006) 102.
[18] B. Liu, W.C. Wang, X.R. Zhang, Phys. Chem. Chem. Phys. 6 (2004) 3985.
[19] P.I. Ravikovitch, G.L. Haller, A.V. Neimark, Adv. Colloid Interface Sci. 76 (1998) 203.
[20] A.V. Neimark, P.I. Ravikovitch, A. Vishnyakov, Phys. Rev. E 62 (2000) R1493.
[21] A.V. Neimark, P.I. Ravikovitch, Charact. Porous Solids V 128 (2000) 51.
[22] P.I. Ravikovitch, S.C. ODomhnaill, A.V. Neimark, F. Schüth, K.K. Unger, Langmuir 11 (1995) 4765.
[23] A.V. Neimark, P.I. Ravikovitch, M. Grun, F. Schüth, K.K. Unger, J. Colloid Interface Sci. 207 (1998) 159.
[24] K.S.W. Sing, D.H. Everett, R.A.W. Haul, L. Moscou, R.A. Pierotti, J. Rouquerol, T. Siemieniewska, Pure Appl. Chem. 57 (1985) 603.
[25] D.W. Sindorf, G.E. Maciel, J. Am. Chem. Soc. 103 (1981) 4263.
[26] M. Pursch, L.C. Sander, K. Albert, Anal. Chem. 68 (1996) 4107.
[27] O.H. Han, Y.K. Bae, S.Y. Jeong, Bull. Korean Chem. Soc. 29 (2008) 405.
[28] W. Gao, L. Reven, Langmuir 11 (1995) 1860.
[29] L.Q. Wang, J. Liu, G.J. Exarhos, K.Y. Flanigan, R. Bordia, J. Phys. Chem. B 104 (2000) 2810.
[30] O.H. Han, Y. Paik, Y.S. Moon, S.K. Lee, T.Y. Kim, Y.H. Lee, W.I. Lee, Chem. Mater. 19 (2007) 3615.
[31] J. Liu, Y. Shin, Z.M. Nie, J.H. Chang, L.Q. Wang, G.E. Fryxell, W.D. Samuels, G.J. Exarhos, J. Phys. Chem. A 104 (2000) 8328.
[32] A.E. Tonelli, F.C. Schilling, Acc. Chem. Res. 14 (1981) 233.
[33] C.R. Kessel, S. Granick, Langmuir 7 (1991) 532.
[34] R. Anwander, I. Nagl, M. Widenmeyer, G. Engelhardt, O. Groeger, C. Palm, T. Roser, J. Phys. Chem. B 104 (2000) 3532.
[35] P.A. Bianconi, F.C. Schilling, T.W. Weidman, Macromolecules 22 (1989) 1697.
[36] R.G. Snyder, M.W. Poore, Macromolecules 6 (1973) 708.
[37] A. Badia, L. Cuccia, L. Demers, F. Morin, R.B. Lennox, J. Am. Chem. Soc. 119 (1997) 2682.
[38] G. Srinivasan, M. Pursch, L.C. Sander, K. Müller, Langmuir 20 (2004) 1746.
[39] N. Sheppard, J. Chem. Phys. 17 (1949) 74.
[40] G.J. Szasz, N. Sheppard, D.H. Rank, J. Chem. Phys. 16 (1948) 704.
[41] J.J. Fox, A.E. Martin, Proc. R. Soc. Lond. Ser. A-Math. Phys. Sci. 175 (1940) 0208.
[42] R.G. Snyder, J. Chem. Phys. 47 (1967) 1316.
[43] M. Maroncelli, S.P. Qi, H.L. Strauss, R.G. Snyder, J. Am. Chem. Soc. 104 (1982) 6237.
[44] R.G. Snyder, M. Maroncelli, S.P. Qi, H.L. Strauss, Science 214 (1981) 188.
[45] J.J. Fox, A.E. Martin, Proc. R. Soc. Lond. Ser. A-Math. Phys. Sci. 167 (1938) 0257.
[46] L.C. Sander, J.B. Callis, L.R. Field, Anal. Chem. 55 (1983) 1068.
[47] J.M. Chalmers, P.R. Griffiths, Handbook of Vibrational Spectroscopy, Wiley, Chichester, 2002.
[48] S. Morita, Y. Ozaki, I. Noda, Appl. Spectrosc. 55 (2001) 1622.
[49] G. Srinivasan, L.C. Sander, K. Müller, Anal. Bioanal. Chem. 384 (2006) 514.
[50] H.L. Casal, H.H. Mantsch, Biochim. Biophys. Acta 779 (1984) 381.
[51] Y.F. Cheng, T.H. Walter, Z.L. Lu, P. Iraneta, B.A. Alden, C. Gendreau, U.D. Neue, J.M. Grassi, J.L. Carmody, J.E. O'Gara, R.P. Fisk, LC GC N. Am. 18 (2000) 1162.